Neuron
Article

Correlated Variability in Laminar Cortical Circuits

Bryan J. Hansen,[1,2] Mircea I. Chelaru,[1,2] and Valentin Dragoi[1,*]
[1]Department of Neurobiology and Anatomy, University of Texas-Houston Medical School, Houston, TX 77030, USA
[2]These authors contributed equally to this work
*Correspondence: valentin.dragoi@uth.tmc.edu
http://dx.doi.org/10.1016/j.neuron.2012.08.029

SUMMARY

Despite the fact that strong trial-to-trial correlated variability in responses has been reported in many cortical areas, recent evidence suggests that neuronal correlations are much lower than previously thought. Here, we used multicontact laminar probes to revisit the issue of correlated variability in primary visual (V1) cortical circuits. We found that correlations between neurons depend strongly on local network context—whereas neurons in the input (granular) layers showed virtually no correlated variability, neurons in the output layers (supragranular and infragranular) exhibited strong correlations. The laminar dependence of noise correlations is consistent with recurrent models in which neurons in the granular layer receive intracortical inputs from nearby cells, whereas supragranular and infragranular layer neurons receive inputs over larger distances. Contrary to expectation that the output cortical layers encode stimulus information most accurately, we found that the input network offers superior discrimination performance compared to the output networks.

INTRODUCTION

It has long been reported that nearby cells in many cortical areas exhibit correlated trial-to-trial response variability (referred to as "noise" correlations), possibly originating from common synaptic input (Bair et al., 2001; Kohn and Smith, 2005; Shadlen and Newsome, 1998). Estimation of correlated neuronal firing is fundamental for understanding how populations of neurons encode sensory inputs. Indeed, the structure of correlations across a network has been shown to influence the available information in the responses of a population of cells (Abbott and Dayan, 1999; Sompolinsky et al., 2001; Cafaro and Rieke, 2010) and possibly limit behavioral performance (Abbott and Dayan, 1999; Cohen and Newsome, 2008). In addition, correlations between neurons can serve to constrain the possible schemes employed by the cortex to code and decode sensory stimuli depending on the stimulus or behavioral context (Ahissar et al., 1992; Cohen and Newsome, 2008; Gutnisky and Dragoi, 2008; Kohn and Smith, 2005; Komiyama et al., 2010; Poulet and Petersen, 2008; Vaadia et al., 1995).

Recently, the issue of correlated neuronal activity has been challenged by experimental evidence (Ecker et al., 2010; Renart et al., 2010) describing spike count correlations in sensory cortex on the order of 10^{-2}. It can be argued that a decorrelated state of the cortex would be advantageous for information processing by reducing the number of neurons necessary to achieve highly accurate network performance (Abbott and Dayan, 1999; Averbeck and Lee, 2004; Ecker et al., 2010; Shadlen and Newsome, 1998). Clearly, elucidating whether cortical networks operate in a correlated or decorrelated state is fundamental for understanding how neuronal populations encode information.

We reasoned that because responses of cortical neurons are significantly influenced by the inputs from other neurons in their local network, correlations may depend on the network environment in which neurons are embedded. Thus, it is widely acknowledged that the structure of local networks depends on cortical layer. Examining how networks in different layers of the cerebral cortex encode information is fundamental for understanding how brain circuits process sensory inputs. Indeed, cortical layers are ubiquitous structures throughout neocortex (Douglas and Martin, 2004; Hubel and Wiesel, 1968; Nassi and Callaway, 2009) consisting of highly recurrent networks (Gilbert and Wiesel, 1983) characterized by distinct connection patterns. Although in recent years significant progress has been made in our understanding of coding strategies across cortical layers (Hansen and Dragoi, 2011; Lakatos et al., 2009; Maier et al., 2010; Opris et al., 2012), there is still a great deal to learn about whether and how neuronal populations encode information in a layer-specific manner.

Our central hypothesis is that the strength of noise correlations depends on cortical layer. Indeed, because the main source of correlations is common input, one would expect that differences in the source and strength of inputs to neurons in different cortical layers would cause changes in correlations. For instance, one important distinction between cortical networks in the middle and superficial and deep layers is the spatial spread of intracortical connections. In the granular layers, where neurons receive geniculate input, the spatial spread of connections is small (Adesnik and Scanziani, 2010; Briggs and Callaway, 2005; Gilbert and Wiesel, 1983), whereas in supragranular and infragranular layers neurons receive recurrent input from larger distances (up to several mm) via long-range horizontal circuitry (Bosking et al., 1997; Gilbert and Wiesel, 1983; Karube and Kisvárday, 2011; Shmuel et al., 2005; Ts'o et al., 1986). The

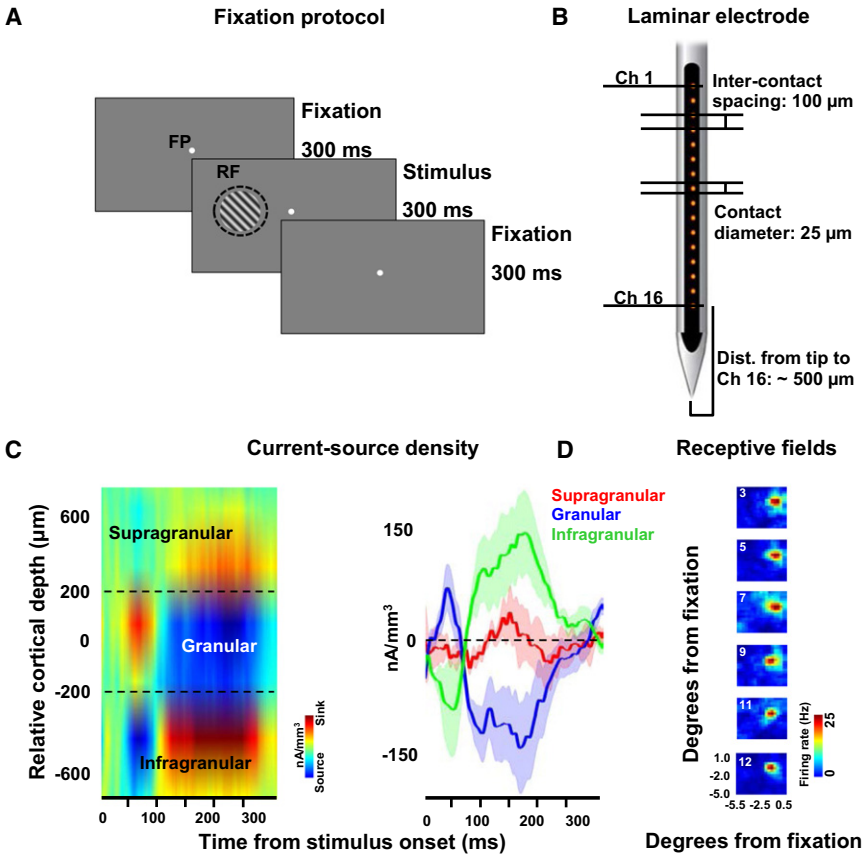

Figure 1. Laminar Recordings and Identification of Cortical Layers

(A) Schematic description of the fixation task protocol. After 300 ms of fixation a sine-wave grating of fixed orientation was presented for 300 ms; after an additional 300 ms of fixation a reward was provided.

(B) Multicontact laminar electrodes were used to record neuronal activity across cortical depth.

(C) Current-source density analysis was used to identify the polarity inversion accompanied by the sink-source configuration at the base of the granular layer. In the example the current sink (shown as red) represents the granular layer and spans ~400 µm. The CSD traces (right) represent the average CSD of those contacts assigned to a given layer.

(D) Receptive fields across contacts were mapped using oriented stimuli presented in random patches. Firing rates for each neuron are calculated independently at 5 ms intervals and the maximum firing rates (shown as red) were used to computed the centroid for each time delay. The time delay with the minimum distance between the centroid and adjacent firing rate locations is chosen as the receptive field.

(E) Two representative examples of spike waveforms isolated on the same channel. Each dot in the scatter plots corresponds to the waveform of one spike from one laminar recording site, giving the coefficient of the first principal component on the x axis and the coefficient of the second principal component on the y axis. The average spike waveforms are shown in solid line; standard deviations are shown in dashed line.

heterogeneity of intracortical inputs to neurons in different cortical layers raises the possibility that pairs of cells may exhibit correlations whose strength varies in a laminar-dependent manner.

RESULTS

Two nonhuman primates (*Macaca mulatta*) performed a fixation task (Figure 1A) while we used multicontact laminar electrodes (Plextrode U-Probe, Plexon; Figure 1B) to record neuronal activity (spikes and local field potentials [LFPs]) at multiple V1 sites of varying cortical depth (n = 544, 16 contacts × 34 sessions). Each electrode consists of 16 equally spaced (100 µm) contacts spanning a total length of 1.6 mm (each contact is 25 µm in diameter and is composed of platinum iridium). Monkeys were required to hold fixation within a 1° window throughout stimulus presentation to earn a juice reward; the trial was automatically aborted if fixation instability exceeded 0.25° at any time during stimulus presentation. While monkeys fixated a white dot in the center of a computer screen, a single oriented grating stimulus was flashed for 300 ms in the center of the neurons' receptive field (5° circular sine-wave gratings with a spatial frequency of 1.4 cycles per degree and a 50% contrast level presented binocularly). The range of stimulus orientation was 0–180° in steps of 22.5° (eight orientations in total) with each orientation randomly presented 50 times across trials (400 trials in total). After the stimulus was extinguished, an additional 300 ms of fixation was required before the monkey was rewarded for maintaining fixation throughout the entire trial. We examined the laminar dependence of fluctuations in neuronal responses, or "noise," by measuring spike count correlations (r_{SC}) between pairs of neurons in the same layer (see Experimental Procedures).

Identification of Cortical Layers

To identify cortical layers, we measured the evoked response potentials (ERPs) from LFPs across equally spaced contacts (100 µm intercontact distance) in response to a full-field flashed stimulus. We then performed current-source density (CSD) analysis (Figure 1C, left) of the LFP time series (according to the

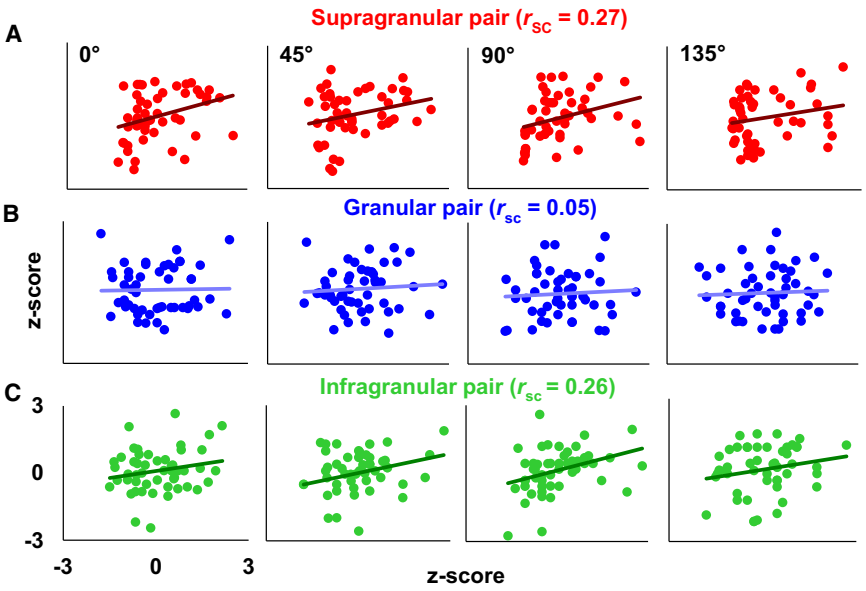

Figure 2. Layer-Dependent Changes in Spike Count Correlations

(A–C) Each scatter plot represents the *Z* score–transformed responses for three example pairs of cells recorded simultaneously in supragranular (A), granular (B), or infragranular (C) layers during the presentation of a particular stimulus orientation (columns: 0°, 45°, 90°, and 135°). The trend line represents the linear regression fit for each pair of cells; r_{SC} for each layer represents the Pearson correlation coefficient extracted from all eight stimulus orientations.

See also Figure S1.

second spatial derivative) to identify the polarity inversion accompanied by the sink-source configuration at the base of layer 4 (the sink is inside layer 4, subsequently referred to as the granular layer) (Hansen and Dragoi, 2011; Hansen et al., 2011; Maier et al., 2010; Schroeder et al., 1998). The CSD traces shown on the right of Figure 1C represent the average of those contacts assigned to a given layer—in this example, the granular layer undergoes a clear increase in CSD amplitude at ~50 ms. Current-source density analysis allowed us to accurately position electrodes to record from all layers in a single penetration while providing an index of the location, direction, and density of transmembrane current flow. This analysis served as a reference to assign electrode contacts above and below the granular (G) layer to supragranular (SG) and infragranular (IG) layers, respectively (the contact with the largest sink center-of-mass served as the granular layer reference at 0 μm; see Experimental Procedures).

We observed that cells recorded on laminar probes had highly overlapping receptive fields (Figure 1D) and highly similar preferred orientations (PO) (e.g., the difference in PO for over 58% of the pairs of neurons was within 0°–10° range, $p < 0.01$, Wilcoxon signed-rank test). Single-unit isolation on the laminar electrode was performed manually, and distinct clusters were identified based on principal component analysis (PCA), as well as spike waveform properties such as, spike width, valley, and peak. Figure 1E contains two representative examples of spike waveforms isolated on the same channel and plotted according to the weight of the first and second principal components. Clusters that clearly separated from the origin of the PCA plot and from other clusters were considered single units (e.g., "Unit a" and "Unit b" in both examples).

Layer-Dependent Changes in Correlated Variability

We collected data from 34 sessions in two monkeys (Monkey W, 27 sessions; Monkey P, 7 sessions) and were able to isolate 199 single units (Monkey W, SG: 54, G: 57, IG: 47; Monkey P, SG: 12, G: 11, IG: 18) that exhibited significant response modulation by stimulus orientation (responses were measured throughout the entire 300 ms period of stimulus presentation). We computed noise correlations for our population of 327 pairs of neurons, assigned to different cortical layers (Monkey W, SG: 91, G: 98, IG: 74; Monkey P, SG: 22, G: 16, IG: 26). Given that our laminar probes were able to record single units from the same cortical column in a single vertical penetration, we expected the amount of common input shared by a pair of neurons to be relatively similar. As a result, we expected strong spike count correlations between nearby cells in each cortical layer.

Figures 2A–2C shows example scatter plots of *Z* score-transformed responses for pairs of cells recorded in different layers during the presentation of specific oriented gratings (0°, 45°, 90°, and 135°; see also Figure S1 available online). Surprisingly, whereas the supragranular (Figure 2A) and infragranular (Figure 2C) layer pairs showed high noise correlations regardless of stimulus orientation (SG, mean correlation 0.27; IG, mean correlation 0.26), the pair in the granular layer (Figure 2B) showed almost no correlated variability across orientations (G, mean correlation 0.05). These results were confirmed across our population of 327 pairs—we found that correlated variability in the supragranular layers was 0.24 ± 0.03 (mean ± SEM), similar to the values previously reported in V1 (Bair et al., 2001; Gutnisky and Dragoi, 2008; Kohn and Smith, 2005; Nauhaus et al., 2009; M.A. Smith and A. Kohn, 2009, Soc. Neurosci., abstract). Out of 113 correlation coefficients, 93 (82.3%) were significantly different from zero ($\alpha = 0.05$, two-sample t test; positive 75.2%, negative 7.1%; statistical significance was assessed by shuffling trials). However, in the granular layer, the mean correlation value was exceedingly low (0.04 ± 0.01), with only 22 statistically significant correlation coefficients out of 114 (19.2%; two-sample t test; positive 12.2%, negative 7.0%), consistent with recent reports in V1 and somatosensory cortex (Ecker et al., 2010; Renart et al., 2010).

In infragranular layers, the value of correlated variability was high again and comparable to that found in supragranular layers (0.23 ± 0.02; out of 100 pairs, 79 had correlation coefficients significantly different from zero; $\alpha = 0.05$, two-sample t test; positive 74%, negative 5%). Figure 3A summarizes the results

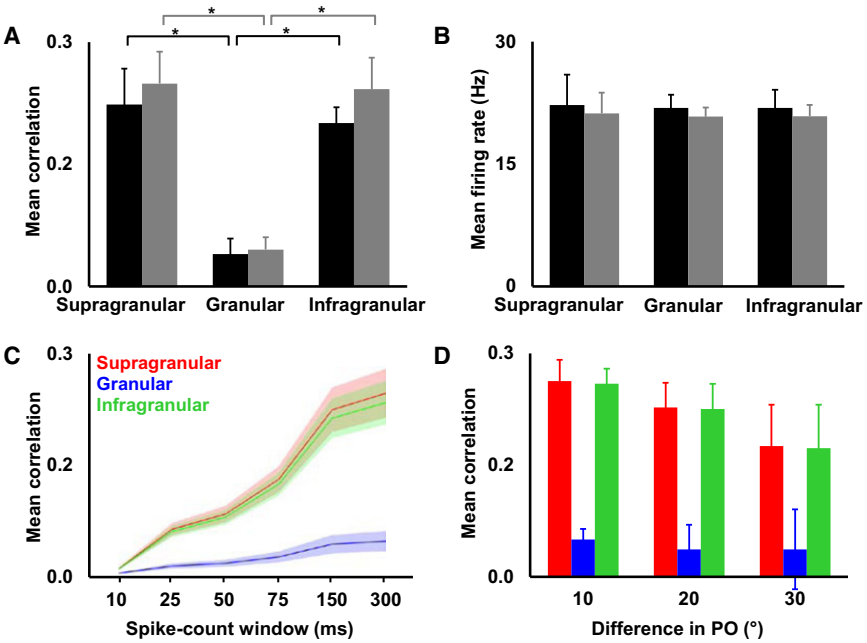

Figure 3. Spike Count Correlation Analysis for the Population of Cell Pairs

(A) Laminar-dependent noise correlations for each of the monkeys used in the experiments (Monkey W, SG: 0.24 ± 0.04, G: 0.04 ± 0.01, IG: 0.24 ± 0.04, black bars; Monkey P, SG: 0.22 ± 0.04, G: 0.04 ± 0.02, IG: 0.2 ± 0.02, gray bars).

(B) Firing rate analysis; mean firing rates do not depend on cortical layer. Each bar represents the average firing rate of the cells recorded in the corresponding cortical layer for the two different monkeys (Monkey W, black bars; Monkey P, gray bars).

(C) Timescale of laminar noise correlations using a range of spike-count windows we observed a steady increase in the mean correlation coefficient in all layers. Shaded envelopes represent SEM.

(D) Layer-dependent mean correlation coefficient as a function of the difference in PO between the neurons in a pair. For the majority of pairs (191/327, 58.4%), the orientation preference difference was within 10° (one-way ANOVA, F (2, 188) = 16.11, $p = 10^{-7}$), whereas in the remaining pairs, 41.6% were characterized by a $\Delta\theta$ range between 10°–30°.

See also Figure S2.

obtained in each monkey—the laminar dependence of noise correlations was consistent across animals (Monkey W, SG: 0.24 ± 0.04, G: 0.04 ± 0.01, IG: 0.24 ± 0.04; Monkey P, SG: 0.22 ± 0.04, G: 0.04 ± 0.02, IG: 0.2 ± 0.02). We also observed a significant difference in mean correlations across layers for each monkey (Monkey W, one–way ANOVA, F (2, 260) = 14.1, $p < 10^{-6}$; Monkey P, one-way ANOVA, F (2, 61) = 8.92, $p < 0.0004$). It should be noted that the cells that we recorded using laminar probes have strong signal correlations (i.e., they prefer the same stimulus orientation as they lie within the same functional column). Therefore, it is not surprising that the correlation values in the SG and IG layers were higher than the mean correlation values reported in previous V1 studies performed using multi-electrode arrays (Gutnisky and Dragoi, 2008; Kohn and Smith, 2005). Interestingly, we failed to find a laminar dependence of noise correlations during the spontaneous activity measured before stimulus presentation ($p > 0.1$, Kruskal-Wallis analysis).

In principle, the laminar differences in noise correlations might have been due to differences in firing rates of the pairs across cortical layers. Indeed, it has been suggested (de la Rocha et al., 2007) that spike count correlations are positively correlated with the mean responses of the cells in a pair (see Bair et al., 2001; Gutnisky and Dragoi, 2008; Kohn and Smith, 2005; Nauhaus et al., 2009). However, we found that the mean firing rates of the cells in our population did not differ across cortical layers in either animal (Figure 3B; population result: one-way ANOVA, F (2, 324) = 0.36, $p > 0.69$). Although other groups have reported systematic differences in firing rates across layers (Snodderly and Gur, 1995), higher firing was typically observed in layers 3B, 4C, and 5 (Ringach et al., 2002), and all layers were characterized by a high diversity of tuning width and spontaneous firing (Ringach et al., 2002; see also Schiller et al., 1976). Unfortunately, the relatively large spacing between our electrode contacts (100 μm) made it difficult to accurately assign single units to individual cortical sublayers. We also observed that, again within each layer, noise correlations did not depend on the geometric mean firing rates of the cells in a pair (SG: $R = -0.07$; G: $R = -0.01$; IG: $R = -0.03$).

Are laminar differences in noise correlations preserved when the timescale at which correlations are measured varies? Indeed, previous studies have shown that noise correlations depend on the precise timescale at which spike rates are counted (Kohn and Smith, 2005). We addressed this issue by recalculating spike count correlations for varying spike count windows during stimulus presentation. Figure 3C summarizes our results: although the mean correlation coefficient increased in all layers as the time window approached the stimulus duration, correlation values in the granular layer continued to remain significantly lower than those in supragranular and infragranular layers (one-way ANOVA, $p < 10^{-6}$). This result indicates that the laminar differences in noise correlations are pronounced even when shorter spike count windows are used to measure correlations.

One variable that is known to influence the strength of noise correlations is signal correlations (Bair et al., 2001; Cohen and Kohn, 2011; de la Rocha et al., 2007; Gutnisky and Dragoi, 2008; Nauhaus et al., 2009). In principle, our use of laminar probes should ensure single–unit recording within individual orientation columns. Therefore, the neurons in each laminar population are expected to be characterized by small differences in their preferred orientation ($\Delta\theta$), which is equivalent to high signal correlations. However, we cannot exclude that the pairs in the granular layers might have been characterized by greater $\Delta\theta$s (equivalent to lower signal correlations) than those in supragranular and infragranular layers. In order to completely rule out this confounding variable (signal correlations), we

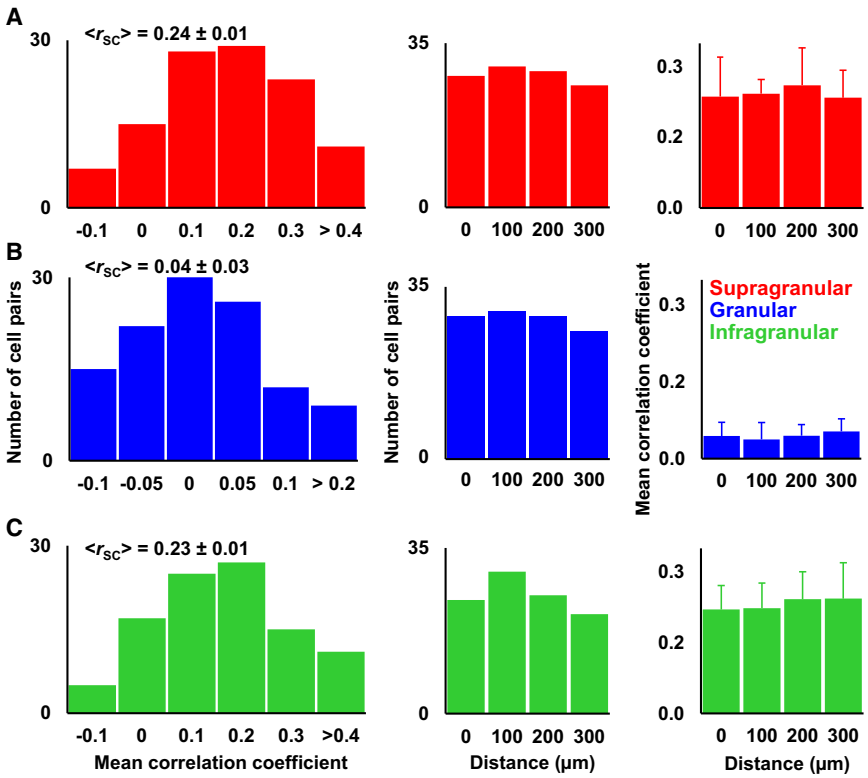

Figure 4. Laminar Distribution and the Effect of Contact Distance on Correlated Variability

(A) Distribution of r_{SC} values for each cortical layer. Although correlation coefficients in infragranular and supragranular layers are skewed toward high values, those in the granular layer have much lower values. The average correlation coefficient for all the pairs in our population (irrespective of cortical layer) is r_{SC} = 0.17.

(B) We computed the percentage of pairs corresponding to each pair distance across layers and observed that ~78% of all the cell pairs were within 200 μm.

(C) Computing the distance between cell pairs we observed that r_{SC} does not depend on contact distance irrespective of cortical layer.

See also Figure S3.

computed the difference in PO between the neurons in a pair using the vector averaging method. For the majority of pairs (191/327, 58.4%), Δθ was within 10° (the remaining pairs were characterized by Δθs between 10°–30°). This indicates that the advancement of the laminar electrode remained isolated to a single cortical column in V1. In Figure 3D, we represented the mean noise correlation in each cortical layer as a function of Δθ and found highly consistent laminar differences in mean correlations. That is, we found a significant laminar difference in noise correlations for pairs with Δθ between 0°–10° (one–way ANOVA, $F(2, 188) = 16.11$, $p = 10^{-7}$). Subsequent multicomparison analysis revealed that the mean correlation of SG and IG pairs was significantly different from the mean correlation of G pairs (Tukey's least significant difference); consistent results were also observed for those pairs with Δθ between 10°–20° ($p = 0.008$) and 20°–30° ($p = 0.05$).

Other neuronal response properties, such as the shape of neurons' tuning curves and reliability of responses, may cause changes in signal correlations to possibly influence the amplitude of noise correlations. We addressed this issue by computing the orientation selectivity index (OSI) (Dragoi et al., 2000; Gutnisky and Dragoi, 2008) and Fano factor (variance/mean) across layers. Although cells in the granular layers tended to have broader orientation selectivity (OSI was decreased by 15% and 11% relative to SG and IG, respectively), consistent with earlier reports (Hubel and Wiesel, 1968; Blasdel and Fitzpatrick, 1984), these changes were not statistically significant (one-way ANOVA, $F(2, 127) = 2.01$, $p = 0.14$). These results are in agreement with a previous report by Ringach et al. (2002) observing only minimal differences in tuning strength across cortical layers, but a high diversity of tuning width and spontaneous firing in all layers (see also Schiller et al., 1976). Analysis of the reliability of neuronal responses, or Fano factor, yielded similar results across layers, with only a slight tendency for neurons in the granular layer to exhibit decreased values ($p > 0.1$, Wilcoxon sign-ranked test). Altogether, these analyses argue that the shape of orientation tuning curves and response reliability cannot explain the laminar dependence of noise correlations.

Figure 4A shows the laminar distribution of correlations—whereas correlation coefficients in supragranular and infragranular layers are skewed toward high values, those in the granular layer have much lower values. Based on our CSD-defined laminar regions, we were able to record from pairs of cells in a given layer up to 400 μm away, and hence investigated the effect of distance between laminar contacts on correlated variability. By computing the number of cell pairs as a function of electrode contact distance across layers, we found that ~78% of cell pairs were within 200 μm (Figure 4B). In addition, the mean correlation coefficient did not depend on contact distance irrespective of cortical layer (Figure 4C; $p > 0.45$; Wilcoxon rank sum test).

We also calculated noise correlations for neuron pairs originating from different layers and found that correlations between neurons in the granular layer and those in other cortical layers (SG-G: 0.12 ± 0.03; IG-G: 0.10 ± 0.03) were significantly weaker. When we computed correlations between neurons in supragranular and infragranular layers we observed significantly higher values (SG-IG: 0.21 ± 0.03; one-way ANOVA, $F(2, 156) = 12.73$, $p = 10^{-5}$; post hoc multicomparison, Tukey's least significant difference). This result is consistent with our hypothesis that there is a greater fraction of common input in the output layers possibly due to the influence of long-range horizontal connections (see Figure S2 for a summary of inter-layer r_{SC}).

The Effects of Eye Movements on Noise Correlations

One possible confound is eye movements during fixation. Indeed, eye movements could modulate the firing rates of all the neurons recorded simultaneously to possibly increase correlated variability due to an increase in common input. Although the eye movement modulation of firing rates has not been demonstrated to depend on cortical layer, one cannot totally exclude the possibility that this modulation could be larger in supragranular and infragranular layers of V1 to contribute to an increase in noise correlations. However, if eye movements were a confounding variable in our study, they would equally affect correlations in all layers. Yet, we report noise correlations that are much smaller in the granular layer. To directly address the issue of eye movements, we examined how the amplitude and velocity of microsaccades affect noise correlations in each cortical layer. For a given session, we computed the amplitude and velocity of eye movements (x and y) during the entire stimulus presentation (300 ms) on a trial-to-trial basis. However, whereas removing trials with both large amplitude and high velocity eye movements slightly reduced the mean correlation coefficients, their laminar dependence was preserved (Figure S3; one-way ANOVA, $p = 10^{-7}$).

A Network Model of Layer-Dependent Neuronal Correlations

What type of layer-specific connectivity pattern would be consistent with the weak spike count correlations in the granular layer but strong correlations in superficial and deep layers? We reasoned that one important distinction between cortical networks in the middle and superficial and deep layers is the spatial spread of intracortical connections. In the granular layers, where neurons receive geniculate input, the spatial spread of connections is small (Adesnik and Scanziani, 2010; Briggs and Callaway, 2005; Gilbert and Wiesel, 1983) whereas in supragranular and infragranular layers neurons receive recurrent input from larger distances (up to several mm) via horizontal and feedback circuitry (Bosking et al., 1997; Gilbert and Wiesel, 1983; Shmuel et al., 2005; Ts'o et al., 1986). The differential spatial spread of intracortical inputs in each cortical layer is likely to affect the orientation distribution of common inputs to cortical neurons. For instance, because long-range horizontal connections preferentially target iso-oriented cells (Blakemore and Tobin, 1972; Gilbert and Wiesel, 1983; Nelson and Frost, 1978), they are likely to sharpen the orientation tuning of excitatory and inhibitory intracortical inputs (i.e., a larger fraction of inputs will originate from iso-oriented cells). Therefore, we reasoned that the unique spatial spread of intracortical inputs in each cortical layer would influence the amount of common input and, as a result, the correlation structure across laminar circuits.

We tested the relationship between the spatial spread of intracortical connections and neuronal correlations by implementing a recurrent network consisting of two populations of excitatory (*E*) and inhibitory (*I*) spiking neurons both receiving excitatory feedforward projections (Figure 5 and Supplemental Experimental Procedures). The connection probability varies with the difference between the neurons' preferred orientations (Figure S4A), i.e., inhibitory inputs to a cortical neuron originate from a broader range of orientations than excitatory inputs (Hirsch et al., 2003; Swadlow, 2003). Despite this difference, the excitatory and inhibitory inputs in all cortical layers are strongest at the preferred orientation of the postsynaptic neuron (Blakemore and Tobin, 1972; Gilbert and Wiesel, 1983; Nelson and Frost, 1978). However, because long-range horizontal connections preferentially target iso-oriented cells, they are likely to sharpen the orientation tuning of excitatory and inhibitory intracortical inputs to neurons in supragranular and infragranular layers.

The orientation tuning of model excitatory and inhibitory inputs to cortical neurons was varied by changing the standard deviation (σ) of the spatial spread of local intracortical connections. To model granular layer we used broadly tuned excitatory and inhibitory inputs, i.e., $\sigma_E = 25^\circ$ for excitatory connections and $\sigma_I = 40^\circ$ for inhibitory connections (Figures 5A and S4A) (Roerig and Chen, 2002; Roerig et al., 2003). In superficial and deep layers, we assumed that the orientation tuning of excitatory and inhibitory currents increases by ~33% (Figure 5B), which corresponds to a 50% reduction of σ_E (Figures S4B and S4E). Figures 5C and 5D illustrate how response correlations start rising when the tuning of excitatory connections becomes narrower (σ_E decreases). For broadly tuned intracortical inputs (Figure 5C), noise correlations are small (10^{-2} magnitude) and relatively evenly distributed around zero irrespective of the difference in orientation. This can be explained by the correlation between the excitatory and inhibitory currents (c_{EI}) that cancel correlations between excitatory-excitatory and inhibitory-inhibitory currents ($c_{EE} + c_{II}$; Figure S4C). Such extremely low noise correlations might indicate that the recurrent network is in an "asynchronous state" in which local excitation is closely tracked by inhibition (Renart et al., 2010). However, as intracortical inputs become more sharply tuned (Figure 5D; $\sigma_E = 12.5^\circ$), correlations start increasing. Indeed, the spatial asymmetry between the excitatory and inhibitory currents (Figure 5A; excitatory currents originate from a nearer pool of cells than inhibitory currents) ensures that c_{EE} and c_{II} increase above c_{EI} to cause an increase in total current correlation (Figure S4D). That is, the orientation asymmetry between excitation and inhibition switches the network from an uncorrelated to a correlated state (Renart et al., 2010). This conclusion is general (Figure 5E), as the orientation spread of excitatory connections decreases relative to the spread of inhibitory connections ($\sigma_E < \sigma_I$), response correlations start rising (Figure 5F). Altogether, these analyses indicate that functional connectivity impacts noise correlations: a broad tuning of intracortical inputs, as in the granular layer, decorrelates responses of nearby neurons, whereas sharper local oriented inputs, as in the supragranular and infragranular layers, cause strong response correlations.

One issue with the analysis in Figure 5 is that it ignores the multilayer structure of V1 cortical networks (Nassi and Callaway, 2009; Douglas and Martin, 2004). How do neurons in the granular layers exhibit low correlated variability despite receiving highly correlated inputs from the deep layers of V1, whereas neurons in the supragranular layers exhibit high correlated variability despite receiving virtually uncorrelated inputs from the granular layer? We addressed this issue by implementing three coupled recurrent networks of excitatory and inhibitory neurons representing the supragranular layers (L2/3), granular layer (L4), and

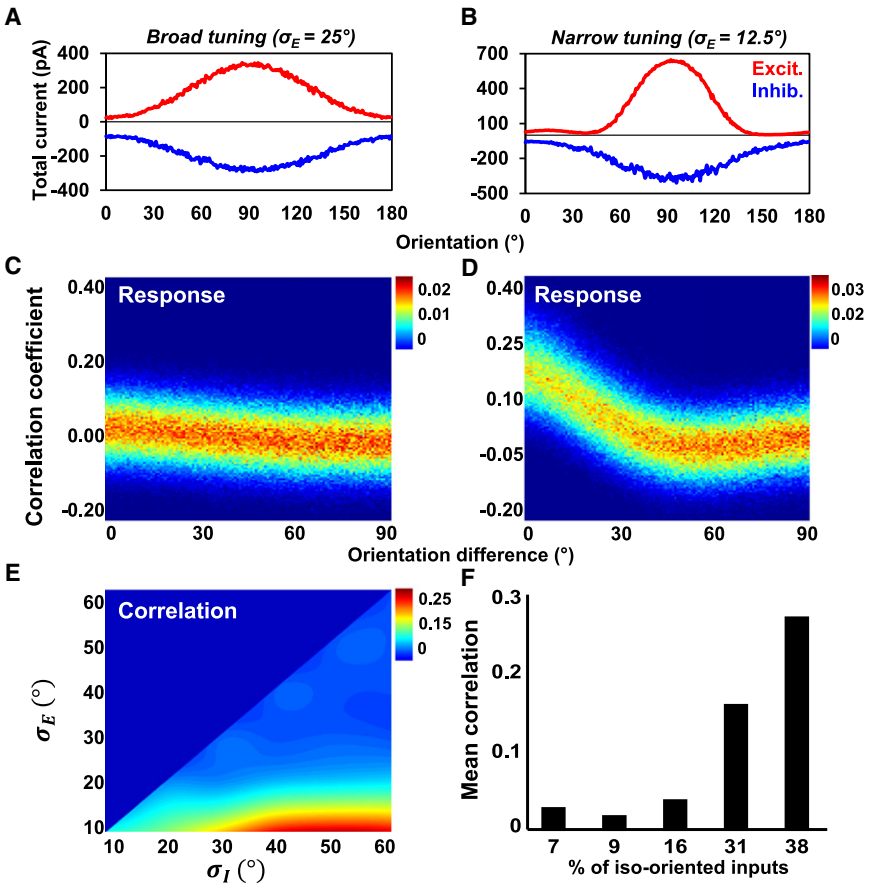

Figure 5. A Recurrent Model that Explores the Mechanism of Layer-Dependent Neuronal Correlations

(A and B) Distribution of total excitatory and inhibitory currents for all the neurons in the network for different values of σ_E when the stimulus is presented at 90°. When excitatory connections are broadly tuned (σ_E = 25°, A), the excitatory and inhibitory current distributions are spatially symmetric; when excitatory connections are narrowly tuned (σ_E = 12.5°, B), there is a spatial asymmetry between the excitatory and inhibitory currents. Each point represents the sum of the incoming excitatory and inhibitory currents for the neuron preferring the orientation marked on the x axis.

(C and D) Probability distribution of response correlations as a function of the orientation difference between the cells in a pair ($\Delta\theta$) for broadly tuned (σ_E = 25°, C) and sharply tuned (σ_E = 12.5°, D) excitatory synaptic inputs.

(E) Peak mean noise correlations computed for different combinations of SDs (σ_E and σ_I) of the excitatory and inhibitory synaptic distributions. For each (σ_E, σ_I) combination, we averaged the noise correlations of all neuronal pairs of similar orientation difference. The largest noise correlations were obtained for small σ_E (10°) and high σ_I (>40°).

(F) Noise correlations increase with the increase of the fraction of iso–oriented inputs (within 5° of the neuron's preferred orientation) to cortical neurons. Mean noise correlations were computed as a function of $\Delta\theta$, and then the peak mean correlation was plotted as a function of the percentage of iso–oriented inputs to cortical neurons (small numbers correspond to a narrow orientation tuning of excitatory synaptic inputs). Error bars represent standard deviation.

See also Figure S4.

infragranular layers (L5/6; Figure 6A, inset). For supragranular and infragranular layers we used a distribution of σ_E = 15° for local intracortical excitatory inputs, σ_I = 40° for local intracortical inhibitory inputs, and σ_E = 20° for feedforward iso-oriented inputs (from granular and supragranular layers, respectively; see Supplemental Experimental Procedures). For the granular layer we used σ_E = 30° for local intracortical excitatory inputs, σ_I = 40° for local intracortical inhibitory inputs, and σ_E = 20° for the inputs from infragranular layers. As shown in Figure 6A, the specific structure of synaptic connectivity within and between layers ensures model mean noise correlations in the 0°–30° orientation range that were highly consistent with experimental data for each layer. Indeed, despite the fact that granular layer neurons receive highly correlated inputs from the infragranular layer, the structure of synaptic connectivity, i.e., the broad tuning of excitatory intracortical inputs, decorrelates responses. In turn, neurons in supragranular layers, where the tuning of excitatory intracortical inputs is narrower, show an increase in correlated variability although their inputs are only weakly correlated. The noise correlation values obtained using our three-layer model are consistent with those obtained experimentally, i.e., correlations in supragranular and infragranular layers are significantly greater than those in the granular layer (one-way ANOVA, $F(2, 115{,}638) = 72{,}346.16$, $p < 0.00001$; post hoc multicomparison, Tukey's least significant difference), but statistically indistinguishable between each other ($p > 0.05$).

Do laminar difference in noise correlations influence the information encoded in population activity in each layer? A measure of the accuracy of population coding is the network discrimination threshold (inversely proportional to the square root of Fisher information) (Abbott and Dayan, 1999), which we computed by using a linear decoder of stimulus orientation (Seriès et al., 2004; Chelaru and Dragoi, 2008). Orientation discrimination performance for each layer was estimated by decoding the spike counts in each layer obtained when bar stimuli of two nearby orientations (90° and 92°) were presented for 504 trials of 0.5 s each (Figure 6B). The decoder was trained to maximize the Fisher information of population responses (Abbott and Dayan, 1999; Seriès et al., 2004; Chelaru and Dragoi, 2008) and, as a result, minimize the discrimination threshold between two adjacent stimulus orientations (Supplemental Experimental Procedures). As expected, we found that the network orientation discrimination threshold is lowest when the population of cells is virtually uncorrelated (granular layer), and is elevated in the supragranular and infragranular layers where correlations are increased (Figure 6B). The discrimination threshold for the granular layer is significantly

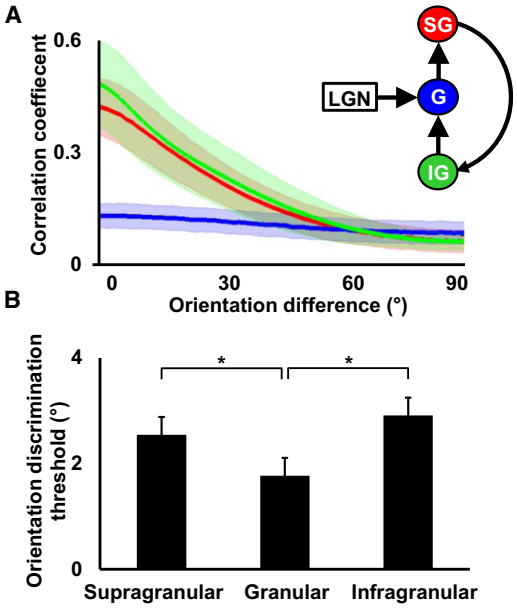

Figure 6. A Recurrent Laminar Network that Explores the Mechanism of Noise Correlations in V1

(A) Noise correlation computed for the supragranular (red) and infragranular layers (green) were significantly higher than correlations in the granular layer (blue) in the 0°–30° orientation difference range. Shaded envelopes represent SD. Inset: V1 microcircuit used to model the functional connectivity between cortical layers. Three recurrent networks were used to model cortical layer 4Cα (granular), layers 2/3 (supragranular), and layers 5/6 (infragranular) respectively. See also Supplemental Experimental Procedures.

(B) Network orientation discrimination threshold, computed using an estimate of Fisher information, was significantly lower for the granular layer compared to supragranular and infragranular layers. The discrimination threshold was not significantly different between the supragranular and infragranular layers. Error bars represent SEM.

smaller ($p < 0.05$, bootstrap method) than that for the supragranular and infragranular layers, but is not significantly different between the supragranular and infragranular layers ($p > 0.05$).

DISCUSSION

A fundamental issue in our understanding of brain circuits is how sensory information is encoded by networks in different layers of the cerebral cortex. In recent years, significant progress has been made in our understanding of coding strategies across cortical layers (Hansen and Dragoi, 2011; Lakatos et al., 2009; Maier et al., 2010; Opris et al., 2012), yet whether and how neuronal populations encode information in a layer-specific manner is virtually unknown. Using laminar recording techniques in combination with evoked-response potentials and current-source density (Hansen et al., 2011) we revisited the issue of correlated variability ("noise" correlations) in V1 circuits. We found that correlations between neurons depend strongly on local network context—whereas neurons in the granular layer showed virtually no correlated variability, neurons in supragranular and infragranular layers exhibited strong response correlations.

Our study potentially sheds light on a recent controversy in the field regarding the issue of correlated variability (Cohen and Kohn, 2011). Thus, despite the fact that strong trial-to-trial correlated variability has long been reported in primary visual cortex (Bair et al., 2001; de la Rocha et al., 2007; Gutnisky and Dragoi, 2008; Kohn and Smith, 2005; Nauhaus et al., 2009), recent evidence from Ecker et al. (2010) has suggested that neuronal correlations are much lower than previously thought. Our study offers experimental evidence in support of the idea that correlations in the granular layer of V1 are an order of magnitude weaker than those in the output layers. Although it is unlikely that Ecker et al. (2010) have recorded solely from the granular layers (they reported a broad range of correlation coefficients), it is entirely possible that a significant number of pairs could have originated from the granular layers. Indeed, electrode arrays used in chronic recordings are often advanced up to 1 mm (within the range of the granular layers) in order to ensure recording stability (Bjornsson et al., 2006). In addition, other factors, such as low mean firing rates due to "oversorting" spike waveforms, could influence the correlation values. Indeed, as shown in Figure 3C, low firing rates (due to small temporal windows) could lead to low correlation coefficients, particularly in the granular layers.

Other experimental variables might have affected the level of correlated variability reported here. For instance, improper spike sorting could inflate correlation coefficients at least by a factor of two by incorrectly measuring correlations between multi-unit, not single-unit, spike counts (Cohen and Kohn, 2011). However, besides the fact that the spike sorting methods used in our study are similar to those used by Ecker et al. (2010), incorrect spike sorting would have affected single-unit isolation in all layers, including granular layers. Therefore, if spike sorting had been an issue in our study, one would have expected noise correlations in the granular layer much higher than those reported in Figure 3A. Another variable affecting noise correlations is eye movements. Microsaccades would be expected to jointly increase or decrease neuronal responses such as to increase correlated variability. However, we found that although noise correlations were decreased somewhat by eliminating the large fixational eye movements, the layer dependency of correlations remained highly significant.

One possible factor that could influence neuronal correlations is the underlying dynamics of cortical responses, or cortical states, due to changes in ongoing rhythmic neural activity. Although we removed the possible contaminating effect of trial-to-trial slow-wave fluctuations in spike counts by performing a "detrending" of individual neuronal responses (Bair et al., 2001), another potential artifact is the rapid, spontaneous, change in rhythmic activity of cortical state (Shaw et al., 1993; van der Togt et al., 2005). Indeed, within-trial rapid changes in cortical state have been shown to affect cross-correlation strength and cross-coherency in different cortical layers (van der Togt et al., 2005), as well as the strength of stimulus-evoked multiple unit responses of V1 neurons. For instance, the highest amplitude multi-unit responses were predominantly found in middle layers of V1 in periods when low-frequency activity increases in magnitude and high-frequency rhythms decrease. Although these rhythmic state-dependent changes in response magnitude could reflect changes in functional connectivity within

V1, they are unlikely to affect the laminar dependency of noise correlations reported here for at least three reasons. First, rhythmic changes in the state of cortical networks have been typically reported in the anesthetized, not awake state of the animal (van der Togt et al., 2005). Second, fluctuations in ongoing activity in the awake state may occur at random times during a trial to possibly affect noise correlations at shorter time scales, but not when spike counts are measured for longer durations (hundreds of ms or more). However, we report here a pronounced laminar dependence of noise correlations at a variety of timescales (Figure 3C). Third, the fact that state-dependent large amplitude responses were mainly observed in layer 4 (van der Togt et al., 2005) would, in principle, be consistent with higher noise correlations in middle layers of V1, which is contrary to the results reported here (low correlations in the granular layer).

The laminar dependency of noise correlations does not necessarily imply that other forms of correlation, such as spike-spike or spike-LFP coherence, would exhibit the same type of layer dependency. Indeed, in one of our recent investigations of rapid adaptation using laminar probes in V1 we found more gamma-band (30–80 Hz) synchronization between individual spikes and LFPs in the granular layer than in deep and superficial layers (Hansen and Dragoi, 2011). However, despite these differences, synchronous gamma-band activity was observed across all layers, unlike the current study revealing the absence of correlated variability in the middle layers of V1. Nonetheless, although measures of noise correlations and synchronization vary significantly in terms of both mathematical formalism and functional implication, they are both measures of local network processing. Indeed, individual neurons in local networks possess increased spike timing synchronization with local field potentials, which may increase network information flow (Fries et al., 2001). It is entirely possible that the same network could exhibit low trial-to-trial correlated variability as a way to reduce network redundancy (Abbott and Dayan, 1999; Averbeck and Lee, 2004; Ecker et al., 2010; Shadlen and Newsome, 1998; Gutnisky and Dragoi, 2008) and increased synchronization in order to improve information flow. This possibility is supported by recent evidence (Womelsdorf et al., 2012) reporting that gamma-band synchronization produces spiking activity that is related to minimal noise correlation in firing rates.

Possible Network Mechanisms

The network mechanism that we described (Figures 5 and 6) predicts that a broad tuning of intracortical inputs, as in the granular layer, decorrelates responses of nearby neurons, whereas a sharper tuning of intracortical inputs due to long-range horizontal connections, as in the supragranular and infragranular layers, causes strong response correlations (i.e., a larger fraction of common inputs will originate from iso-oriented cells). This idea critically rests on experimental evidence that the spatial spread of connections in the granular layers is small, whereas in supragranular and infragranular layers neurons receive recurrent input over larger distances (up to several mm) via horizontal and feedback circuitry. The one-layer model described in Figure 5 represents the extension of a recurrent model recently presented by Renart et al. (2010) showing that an ''asynchronous state'' characterized by low noise correlations emerges spontaneously in cortical circuits when the activity of excitatory and inhibitory populations track each other. The key assumption in the Renart et al. (2010) model is uniform excitatory and inhibitory connection probabilities, (i.e., the probability that two neurons are connected is independent on the neurons' position in the network). We were able to replicate the findings of Renart et al. (2010) (i.e., extremely low noise correlations), when the orientation spreads of excitatory and inhibitory connections were large (>60°) and relatively equal to each other. However, we found that noise correlations are significantly larger than zero in the more realistic scenario in which the tuning of excitatory connections is sharper than that of inhibitory connections.

One could argue that the strength of noise correlations depends critically on model connectivity, including intracortical and interlaminar connections, and that our insufficient knowledge of cortical microcircuit anatomy is unable to constrain the model parameters. Indeed, the precise cortical circuitry of macaque V1 is currently unknown, including the orientation spread of local and long-range excitatory and inhibitory connection, both within and between cortical layers. However, it is unlikely that our modeling results might have been the consequence of particular combinations of parameter values. First, the one-layer model used in the simulations (Figure 5) is a classic recurrent spiking model, with parameter values derived from anatomical and electrophysiological data, that has been extensively used over the past 17 years (Somers et al., 1995; Seriès et al., 2004; Chelaru and Dragoi, 2008). Second, as shown in Figure 5E, when model parameters are held constant, the absolute value of the correlation strength depends on the ratio between the orientation spread of excitatory and inhibitory inputs. Figure 5E demonstrates that our results are robust—for any value of σ_i, noise correlations start rising as σ_E is decreased relative to σ_i, which is exactly our critical assumption. Third, the correlation values depend exclusively on intracortical excitation and inhibition, not on the model interlaminar circuitry, which is identical for each pair of layers. Indeed, it is remarkable that the model granular layer neurons are virtually uncorrelated despite receiving highly correlated inputs from the infragranular layers. In contrast, the supragranular layer neurons are strongly correlated despite receiving uncorrelated inputs from the granular layer. These effects demonstrate the robustness of our model and highlight the importance of intracortical circuitry in shaping the pattern of intracortical correlations.

Although capturing the major interlaminar connectivity in V1, our multilayer model of correlations ignores other aspects of laminar circuitry. For instance, the major recipient of geniculocortical inputs is layer 4C, in which spiny stellate neurons project mostly to layers 2–4B, with only weak projections to L5/6 (Douglas and Martin, 2004; Nassi and Callaway, 2009). A subset of supragranular neurons sends intrinsic projections to neurons in L5. In L6, one class of pyramidal cell receives input from layers 2–4B that synapse on their basal dendrites ramifying in L5, whereas the second class has only few dendritic branches within L5 and provides strong feedback to layer 4C. Although L6 is not capable of driving neurons in layer 4C, it is thought to play a modulatory role (Douglas and Martin, 2004; Nassi and Callaway, 2009). Nonetheless, adding more detailed circuitry to the

three-layer cortical network examined in Figure 6 is unlikely to change our results. Indeed, our model clearly shows that the structure of local excitatory and inhibitory intracortical connections is sufficient to amplify correlations in the supragranular and infragranular layers while reducing them in the granular layers. Because the efficacy of local intracortical connections is unlikely to change depending on input correlations, the local connectivity pattern (specific to each cortical layer) ensures that the results in Figure 6 hold irrespective of the degree of correlation in cortical inputs to each layer.

In principle, other mechanisms besides the layer-specific spread of recurrent connections might be invoked to explain our results. For instance, corticocortical feedback projections from higher cortical areas (Felleman and Van Essen, 1991; Salin and Bullier, 1995) could, at least in principle, explain the effects described here. Indeed, top-down feedback projections have been shown to target L2/3 (our supragranular layer recordings) and L5/6 (infragranular layers; Rockland and Van Hoesen, 1994; Anderson and Martin, 2009; Anderson et al., 2011; Kennedy and Bullier, 1985; Felleman and Van Essen, 1991) while avoiding the granular layer (Angelucci and Bressloff, 2006; Dong et al., 2004). These data might explain some of the difference in correlations between the supragranular and granular layers, as well the emergence of strong correlations in the infragranular layers of V1. However, extrastriate feedback projections primarily carry iso-orientation signals (Gallant et al., 1993), and therefore the mechanism that controls the switch from weak to strong correlations based on differences in the tuning of excitatory intracortical inputs would be similar to that described in our study. Another possible explanation for the low correlated variability in the granular layers is the fact that the LGN inputs targeting granular layer cells may be only weakly correlated. In principle, this mechanism may appear unlikely to fully explain our data as it ignores the fact that neurons in the granular layer receive most of their inputs from intracortical sources, including correlated inputs from infragranular and supragranular layer. In sum, although the laminar dependence of the spatial spread of intracortical inputs appears to be consistent with layer-dependent noise correlations, future experimental and theoretical work is required to precisely determine the mechanism underlying changes in neuronal correlations and their relationship with network performance.

The fact that the laminar structure of correlations revealed experimentally may depend on short and long-range intracortical connectivity in V1 raises the issue of whether similar patterns of connections exist outside V1. Thus, we reviewed studies examining the specificity of local intracortical connections in extrastriate cortex as well as other early sensory cortical areas (e.g., primary auditory cortex [A1] and primary somatosensory cortex [S1]). In area V2 of macaque visual cortex, biocytin-labeled pyramidal neurons of L2/3 and L5 have been shown to provide laterally spreading axon projections that terminate in discrete patches (250–300 μm diameter), primarily in L2/3, and distributed in an elongated field orthogonal to the stripe compartments (Levitt et al., 1994). There were prominent patchy connections within, as well as between, individual compartments, perhaps reflecting functional substructures within stripes. In area V4 of macaque visual cortex, pyramidal neurons of L2/3 make extensive lateral projections with oval or circular patches of terminals in L1–L3 (Yoshioka et al., 1992). It has been reported that any small patch of tissue (~250 μm wide) injected in the superficial layers connects reciprocally to patches scattered up to 3 mm around the injection. In contrast, small injections in L4 did not produce similar patch-like lattice connections, whereas injections in L5 gave relatively weak rising contributions compared to the superficial layer patch system. These findings indicate a functional repeat distance of 450–600 μm in area V4 with a patchy, discontinuous layout.

In addition to visual cortex, other sensory cortical areas are characterized by similar intracortical connectivity patterns. For instance, in cat primary auditory cortex (A1), it has been reported using retrograde anatomic tracing and topographic physiologic mapping of acoustic responses (Read et al., 2001) that L2/3 are characterized by long-range (>1.5 mm) connections between patches with similar acoustic properties, whereas connections in L4 are mostly local. Similarly, L3 of cat primary somatosensory cortex (S1) is characterized by long-range horizontal axons that can travel for up to 2.5 mm (Schwark and Jones, 1989), whereas L4 connections are mostly local. Importantly, long-range horizontal connections in cat S1 are patchy and connect neurons tuned to the same whisker.

Layer-Dependent Population Coding

Surprisingly, we found that populations of neurons in different cortical layers may employ different coding strategies. By operating in a virtually uncorrelated state, cells in the granular layer, which receive afferents from networks in hierarchically lower cortical and subcortical areas, and have only local projections to other layers within V1, may encode incoming stimuli more accurately than cells in the supragranular and infragranular layers (based on the results of our model and using linear decoder analysis). In contrast, the output layers (supragranular and infragranular), which send projections to other cortical and subcortical areas possibly encode information less accurately by exhibiting large correlated variability.

The fact that our results suggest that response decorrelation in the granular layer may be beneficial for sensory discriminations (Figure 6B) raises the issue of whether the higher correlations in supragranular and infragranular layers are detrimental for the information that V1 transmits to other cortical areas. However, this is unlikely to be the case. Indeed, whereas neuronal responses in the granular layer may be optimized for sensory discrimination, the processing of information is mostly local. In contrast, neurons in the supragranular and infragranular layers use long–range cortical projections to process afferent inputs in a context-dependent manner (Adesnik and Scanziani, 2010; Briggs and Callaway, 2005; Gilbert and Wiesel, 1983). Importantly, long-range horizontal connections are essential for performing complex computations, such as contour grouping (Roelfsema et al., 2004) or figure-ground segregation (Salinas and Sejnowski, 2000), which may rely on strong correlations between neurons. Future research will elucidate whether the layer dependence of response correlations is restricted to primary sensory areas or whether it is a component of a more general coding strategy found in downstream cortical areas.

EXPERIMENTAL PROCEDURES

Experimental Paradigm

All experiments were performed in accordance with protocols approved by The Animal Welfare Committee (AWC) and the Institutional Animal Care and Use Committee (IACUC) for the University of Texas Health Science Center at Houston (UTHealth). Two rhesus monkeys (*Macaca mulatta*) performed a fixation task. Monkeys were trained to fixate a small spot (0.1°) presented on a video monitor placed at a distance of 57 cm from each monkey's eye. Stimuli were generated with Psychophysics Toolbox using MATLAB and presented on a 19'' CRT color video monitor (Dell, with a 60 Hz refresh rate). All stimuli were static and consisted of 5° circular sine-wave gratings of random orientation (eight equally spaced orientations spanning 0°–180°; random spatial phase for each orientation; 1.4 cycles per degree spatial frequency and 50% contrast level presented binocularly) flashed in the center of the neurons' receptive fields for 300 ms. Each orientation was randomly presented 50 times. Eye position was continuously monitored using an eye tracker system (EyeLink II, SR Research) with a binocular 1 kHz sampling rate (microsaccades were analyzed every 10 ms by using a vector velocity threshold of 10°/s). Stimulus presentation and eye position monitoring were recorded and synchronized with neuronal data using the Experiment Control Module programmable device (FHC).

Multicontact Electrophysiological Recordings

We conducted 34 recording sessions in two monkeys using laminar electrodes. On average, we were able to identify 16 LFPs and six to ten single units per recording session for each electrode. Each laminar electrode consisted of a linear array of 16 equally spaced contacts (100 μm intercontact spacing) positioned to sample from all cortical layers simultaneously (Plextrode U-Probe, Plexon). Real-time neuronal signals recorded from multiple contacts along the electrode shaft (simultaneous 40 kHz A/D conversion on each channel) were analyzed with a Multichannel Acquisition Processor system (MAP, Plexon).

Current Source Density Analysis

For each recording session, we verified the laminar position of the electrode contacts by computing the evoked potential (ERP) profiles for brief visual stimulation during a passive fixation task (full-field black screen that flashed white for 100 ms, and then returned to black). LFP responses were processed to obtain ERP traces for each contact (over 100 trials). We computed the current source density (CSD) by using the second spatial derivative of the LFP time-series across equally spaced laminar contacts using the iCSD toolbox for MATLAB (Pettersen et al., 2006). We analyzed the laminar CSD profile to verify the presence of a primary sink in the granular layer in each of the 34 recording sessions (the contact with the sink centroid served as granular layer reference at 0 μm). We then analyzed all the contacts above and below the reference and grouped them into one of three possible layers: supragranular, granular, and infragranular (see Supplemental Experimental Procedures).

Noise Correlations

We measured spike count correlations (r_{SC}) between pairs of neurons in different layers. The calculation of r_{SC} for a pair of neurons responding to particular stimulus orientation (θ) is as follows:

$$r_{sc}(\theta) = \frac{\sum_{k=1}^{N}(r_{ik} - r_i)(r_{jk} - r_j)}{N\sigma_i\sigma_j} = \frac{\sum_{k=1}^{N} r_{ik}r_{jk} - r_i r_j}{N\sigma_i\sigma_j}, \quad (1)$$

where N is the number of trials, r_{ik} is the firing rate of neuron i in trial k, r_i is the mean firing rate, and σ_i is the SD of the responses for neuron i (Bair et al., 2001). We transformed the firing rates of neurons into Z scores, $r_{ik} \rightarrow z_{ik} = (r_{ik} - r_i)/\sigma_i$ to eliminate the effect of stimulus orientation on the computation of noise correlations. To compute noise correlations for all stimulus orientations $\{\theta_1, \theta_2, \ldots, \theta_n\}$, we calculated for each neuronal pair the correlations $r_{sc}(\theta_1)$, $r_{sc}(\theta_2), \ldots r_{sc}(\theta_n)$ and then averaged them in order to obtain the noise correlation coefficient for that pair:

$$r_{SC} = E[r_{sc}(\theta_1),\ r_{sc}(\theta_2), \ldots,\ r_{sc}(\theta_n)]. \quad (2)$$

To remove potential artifacts in the calculation of correlation coefficient, such as slow-wave fluctuations in responses across trials, all the neurons underwent detrending in which the spike counts for each trial were high-pass filtered using a linear-phase finite impulse response filter (Bair et al., 2001; Kohn and Smith, 2005).

SUPPLEMENTAL INFORMATION

Supplemental Information includes Supplemental Experimental Procedures, and four figures and can be found with this article online at http://dx.doi.org/10.1016/j.neuron.2012.08.029.

ACKNOWLEDGMENTS

We thank D. Gutnisky and K. Josić for comments on the manuscript and S. Pojoga for assistance during monkey training. This work was supported by grants from NEI, NIH EUREKA Program, Pew Scholars Program, and James S. McDonnell Foundation (V.D.), and an NIH Vision Training Grant (B.J.H).

Accepted: August 8, 2012
Published: November 7, 2012

REFERENCES

Abbott, L.F., and Dayan, P. (1999). The effect of correlated variability on the accuracy of a population code. Neural Comput. *11*, 91–101.

Adesnik, H., and Scanziani, M. (2010). Lateral competition for cortical space by layer-specific horizontal circuits. Nature *464*, 1155–1160.

Ahissar, E., Vaadia, E., Ahissar, M., Bergman, H., Arieli, A., and Abeles, M. (1992). Dependence of cortical plasticity on correlated activity of single neurons and on behavioral context. Science *257*, 1412–1415.

Anderson, J.C., and Martin, K.A. (2009). The synaptic connections between cortical areas V1 and V2 in macaque monkey. J. Neurosci. *29*, 11283–11293.

Anderson, J.C., Kennedy, H., and Martin, K.A. (2011). Pathways of attention: synaptic relationships of frontal eye field to V4, lateral intraparietal cortex, and area 46 in macaque monkey. J. Neurosci. *31*, 10872–10881.

Angelucci, A., and Bressloff, P.C. (2006). Contribution of feedforward, lateral and feedback connections to the classical receptive field center and extra-classical receptive field surround of primate V1 neurons. Prog. Brain Res. *154*, 93–120.

Averbeck, B.B., and Lee, D. (2004). Coding and transmission of information by neural ensembles. Trends Neurosci. *27*, 225–230.

Bair, W., Zohary, E., and Newsome, W.T. (2001). Correlated firing in macaque visual area MT: time scales and relationship to behavior. J. Neurosci. *21*, 1676–1697.

Bjornsson, C.S., Oh, S.J., Al-Kofahi, Y.A., Lim, Y.J., Smith, K.L., Turner, J.N., De, S., Roysam, B., Shain, W., and Kim, S.J. (2006). Effects of insertion conditions on tissue strain and vascular damage during neuroprosthetic device insertion. J. Neural Eng. *3*, 196–207.

Blakemore, C., and Tobin, E.A. (1972). Lateral inhibition between orientation detectors in the cat's visual cortex. Exp. Brain Res. *15*, 439–440.

Blasdel, G.G., and Fitzpatrick, D. (1984). Physiological organization of layer 4 in macaque striate cortex. J. Neurosci. *4*, 880–895.

Bosking, W.H., Zhang, Y., Schofield, B., and Fitzpatrick, D. (1997). Orientation selectivity and the arrangement of horizontal connections in tree shrew striate cortex. J. Neurosci. *17*, 2112–2127.

Briggs, F., and Callaway, E.M. (2005). Laminar patterns of local excitatory input to layer 5 neurons in macaque primary visual cortex. Cereb. Cortex *15*, 479–488.

Cafaro, J., and Rieke, F. (2010). Noise correlations improve response fidelity and stimulus encoding. Nature *468*, 964–967.

Chelaru, M.I., and Dragoi, V. (2008). Efficient coding in heterogeneous neuronal populations. Proc. Natl. Acad. Sci. USA *105*, 16344–16349.

Cohen, M.R., and Kohn, A. (2011). Measuring and interpreting neuronal correlations. Nat. Neurosci. *14*, 811–819.

Cohen, M.R., and Newsome, W.T. (2008). Context-dependent changes in functional circuitry in visual area MT. Neuron *60*, 162–173.

de la Rocha, J., Doiron, B., Shea-Brown, E., Josić, K., and Reyes, A. (2007). Correlation between neural spike trains increases with firing rate. Nature *448*, 802–806.

Dong, H., Wang, Q., Valkova, K., Gonchar, Y., and Burkhalter, A. (2004). Experience-dependent development of feedforward and feedback circuits between lower and higher areas of mouse visual cortex. Vision Res. *44*, 3389–3400.

Douglas, R.J., and Martin, K.A. (2004). Neuronal circuits of the neocortex. Annu. Rev. Neurosci. *27*, 419–451.

Dragoi, V., Sharma, J., and Sur, M. (2000). Adaptation-induced plasticity of orientation tuning in adult visual cortex. Neuron *28*, 287–298.

Ecker, A.S., Berens, P., Keliris, G.A., Bethge, M., Logothetis, N.K., and Tolias, A.S. (2010). Decorrelated neuronal firing in cortical microcircuits. Science *327*, 584–587.

Felleman, D.J., and Van Essen, D.C. (1991). Distributed hierarchical processing in the primate cerebral cortex. Cereb. Cortex *1*, 1–47.

Fries, P., Reynolds, J.H., Rorie, A.E., and Desimone, R. (2001). Modulation of oscillatory neuronal synchronization by selective visual attention. Science *291*, 1560–1563.

Gallant, J.L., Braun, J., and Van Essen, D.C. (1993). Selectivity for polar, hyperbolic, and Cartesian gratings in macaque visual cortex. Science *259*, 100–103.

Gilbert, C.D., and Wiesel, T.N. (1983). Clustered intrinsic connections in cat visual cortex. J. Neurosci. *3*, 1116–1133.

Gutnisky, D.A., and Dragoi, V. (2008). Adaptive coding of visual information in neural populations. Nature *452*, 220–224.

Hansen, B.J., and Dragoi, V. (2011). Adaptation-induced synchronization in laminar cortical circuits. Proc. Natl. Acad. Sci. USA *108*, 10720–10725.

Hansen, B.J., Eagleman, S., and Dragoi, V. (2011). Examining local network processing using multi-contact laminar electrode recording. J. Vis. Exp. http://dx.doi.org/10.3791/2806, September 8, 2011.

Hirsch, J.A., Martinez, L.M., Pillai, C., Alonso, J.M., Wang, Q., and Sommer, F.T. (2003). Functionally distinct inhibitory neurons at the first stage of visual cortical processing. Nat. Neurosci. *6*, 1300–1308.

Hubel, D.H., and Wiesel, T.N. (1968). Receptive fields and functional architecture of monkey striate cortex. J. Physiol. *195*, 215–243.

Karube, F., and Kisvárday, Z.F. (2011). Axon topography of layer IV spiny cells to orientation map in the cat primary visual cortex (area 18). Cereb. Cortex *21*, 1443–1458.

Kennedy, H., and Bullier, J. (1985). A double-labeling investigation of the afferent connectivity to cortical areas V1 and V2 of the macaque monkey. J. Neurosci. *5*, 2815–2830.

Kohn, A., and Smith, M.A. (2005). Stimulus dependence of neuronal correlation in primary visual cortex of the macaque. J. Neurosci. *25*, 3661–3673.

Komiyama, T., Sato, T.R., O'Connor, D.H., Zhang, Y.X., Huber, D., Hooks, B.M., Gabitto, M., and Svoboda, K. (2010). Learning-related fine-scale specificity imaged in motor cortex circuits of behaving mice. Nature *464*, 1182–1186.

Lakatos, P., O'Connell, M.N., Barczak, A., Mills, A., Javitt, D.C., and Schroeder, C.E. (2009). The leading sense: supramodal control of neurophysiological context by attention. Neuron *64*, 419–430.

Levitt, J.B., Yoshioka, T., and Lund, J.S. (1994). Intrinsic cortical connections in macaque visual area V2: evidence for interaction between different functional streams. J. Comp. Neurol. *342*, 551–570.

Maier, A., Adams, G.K., Aura, C., and Leopold, D.A. (2010). Distinct superficial and deep laminar domains of activity in the visual cortex during rest and stimulation. Front. Syst. Neurosci. *4*, pii 31.

Nassi, J.J., and Callaway, E.M. (2009). Parallel processing strategies of the primate visual system. Nat. Rev. Neurosci. *10*, 360–372.

Nauhaus, I., Busse, L., Carandini, M., and Ringach, D.L. (2009). Stimulus contrast modulates functional connectivity in visual cortex. Nat. Neurosci. *12*, 70–76.

Nelson, J.I., and Frost, B.J. (1978). Orientation-selective inhibition from beyond the classic visual receptive field. Brain Res. *139*, 359–365.

Opris, I., Hampson, R.E., Gerhardt, G.A., Berger, T.W., and Deadwyler, S.A. (2012). Columnar processing in primate pFC: evidence for executive control microcircuits. J. Cogn. Neurosci. *24*, 2334–2347.

Pettersen, K.H., Devor, A., Ulbert, I., Dale, A.M., and Einevoll, G.T. (2006). Current-source density estimation based on inversion of electrostatic forward solution: effects of finite extent of neuronal activity and conductivity discontinuities. J. Neurosci. Methods *154*, 116–133.

Poulet, J.F., and Petersen, C.C. (2008). Internal brain state regulates membrane potential synchrony in barrel cortex of behaving mice. Nature *454*, 881–885.

Read, H.L., Winer, J.A., and Schreiner, C.E. (2001). Modular organization of intrinsic connections associated with spectral tuning in cat auditory cortex. Proc. Natl. Acad. Sci. USA *98*, 8042–8047.

Renart, A., de la Rocha, J., Bartho, P., Hollender, L., Parga, N., Reyes, A., and Harris, K.D. (2010). The asynchronous state in cortical circuits. Science *327*, 587–590.

Ringach, D.L., Shapley, R.M., and Hawken, M.J. (2002). Orientation selectivity in macaque V1: diversity and laminar dependence. J. Neurosci. *22*, 5639–5651.

Rockland, K.S., and Van Hoesen, G.W. (1994). Direct temporal-occipital feedback connections to striate cortex (V1) in the macaque monkey. Cereb. Cortex *4*, 300–313.

Roelfsema, P.R., Lamme, V.A., and Spekreijse, H. (2004). Synchrony and covariation of firing rates in the primary visual cortex during contour grouping. Nat. Neurosci. *7*, 982–991.

Roerig, B., and Chen, B. (2002). Relationships of local inhibitory and excitatory circuits to orientation preference maps in ferret visual cortex. Cereb. Cortex *12*, 187–198.

Roerig, B., Chen, B., and Kao, J.P. (2003). Different inhibitory synaptic input patterns in excitatory and inhibitory layer 4 neurons of ferret visual cortex. Cereb. Cortex *13*, 350–363.

Salin, P.A., and Bullier, J. (1995). Corticocortical connections in the visual system: structure and function. Physiol. Rev. *75*, 107–154.

Salinas, E., and Sejnowski, T.J. (2000). Impact of correlated synaptic input on output firing rate and variability in simple neuronal models. J. Neurosci. *20*, 6193–6209.

Schiller, P.H., Finlay, B.L., and Volman, S.F. (1976). Quantitative studies of single-cell properties in monkey striate cortex. II. Orientation specificity and ocular dominance. J. Neurophysiol. *39*, 1320–1333.

Schroeder, C.E., Mehta, A.D., and Givre, S.J. (1998). A spatiotemporal profile of visual system activation revealed by current source density analysis in the awake macaque. Cereb. Cortex *8*, 575–592.

Schwark, H.D., and Jones, E.G. (1989). The distribution of intrinsic cortical axons in area 3b of cat primary somatosensory cortex. Exp. Brain Res. *78*, 501–513.

Seriès, P., Latham, P.E., and Pouget, A. (2004). Tuning curve sharpening for orientation selectivity: coding efficiency and the impact of correlations. Nat. Neurosci. *7*, 1129–1135.

Shadlen, M.N., and Newsome, W.T. (1998). The variable discharge of cortical neurons: implications for connectivity, computation, and information coding. J. Neurosci. *18*, 3870–3896.

Shaw, G.L., Krüger, J., Silverman, D.J., Aertsen, A.M., Aiple, F., and Liu, H.C. (1993). Rhythmic and patterned neuronal firing in visual cortex. Neurol. Res. *15*, 46–50.

Shmuel, A., Korman, M., Sterkin, A., Harel, M., Ullman, S., Malach, R., and Grinvald, A. (2005). Retinotopic axis specificity and selective clustering of

feedback projections from V2 to V1 in the owl monkey. J. Neurosci. *25*, 2117–2131.

Snodderly, D.M., and Gur, M. (1995). Organization of striate cortex of alert, trained monkeys (Macaca fascicularis): ongoing activity, stimulus selectivity, and widths of receptive field activating regions. J. Neurophysiol. *74*, 2100–2125.

Somers, D.C., Nelson, S.B., and Sur, M. (1995). An emergent model of orientation selectivity in cat visual cortical simple cells. J. Neurosci. *15*, 5448–5465.

Sompolinsky, H., Yoon, H., Kang, K., and Shamir, M. (2001). Population coding in neuronal systems with correlated noise. Phys. Rev. E Stat. Nonlin. Soft Matter Phys. *64*, 051904.

Swadlow, H.A. (2003). Fast-spike interneurons and feedforward inhibition in awake sensory neocortex. Cereb. Cortex *13*, 25–32.

Ts'o, D.Y., Gilbert, C.D., and Wiesel, T.N. (1986). Relationships between horizontal interactions and functional architecture in cat striate cortex as revealed by cross-correlation analysis. J. Neurosci. *6*, 1160–1170.

Vaadia, E., Haalman, I., Abeles, M., Bergman, H., Prut, Y., Slovin, H., and Aertsen, A. (1995). Dynamics of neuronal interactions in monkey cortex in relation to behavioural events. Nature *373*, 515–518.

van der Togt, C., Spekreijse, H., and Supèr, H. (2005). Neural responses in cat visual cortex reflect state changes in correlated activity. Eur. J. Neurosci. *22*, 465–475.

Womelsdorf, T., Lima, B., Vinck, M., Oostenveld, R., Singer, W., Neuenschwander, S., and Fries, P. (2012). Orientation selectivity and noise correlation in awake monkey area V1 are modulated by the γ cycle. Proc. Natl. Acad. Sci. USA *109*, 4302–4307.

Yoshioka, T., Levitt, J.B., and Lund, J.S. (1992). Intrinsic lattice connections of macaque monkey visual cortical area V4. J. Neurosci. *12*, 2785–2802.